FORMATION AND ARCHITECTURE OF THE MULTI-STAGE PEACE VALLIS ALLUVIAL FAN SYSTEM, GALE CRATER, MARS.

Z. E. Gallegos[1], H. E. Newsom[1], L. A. Scuderi[1], R. C. Wiens[1], J. A. Grant[2], O. Gasnault[3], S. LeMoulic[4], S. E. Johnstone[1]. [1]Earth and Planetary Science Dept., Institute of Meteoritics, Univ. of New Mexico. (zeg@unm.edu), [2]Center for Earth and Planetary Studies, National Air and Space Museum, Smithsonian Institution, [3]Institut de Recherche en Astrophysique et Planétologie (IRAP),[4]CNRS Université de Nantes.

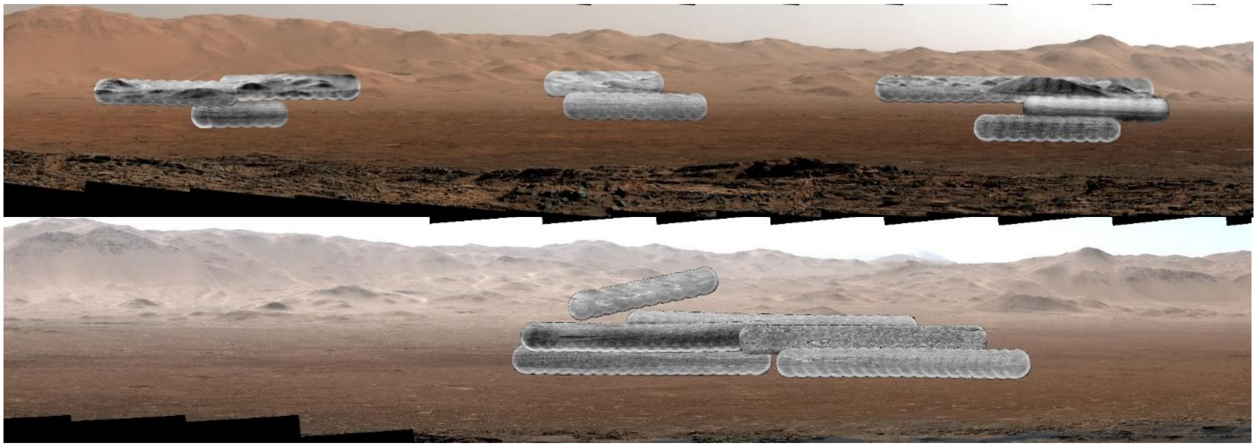

Figure 1. *Top*: Mastcam panorama (sol 1284) with ChemCam RMI mosaics (sols 1241-1311) from the head and flanks of the Peace Vallis fan during Phase 1 of the Peace Vallis campaign. *Bottom*: Mastcam panorama (sol 1950) with ChemCam RMI mosaics (sols 1981-2012) from the head to the foot of the central section of the Peace Vallis fan during Phase 2 of the Peace Vallis campaign.

Introduction: Using a combination of rover imagery and orbital data, the Peace Vallis alluvial fan is reevaluated with regard to the formation and sedimentary architecture of this complex fan system. Original interpretations provided the initial groundwork for understanding textural differences between various units [1,2], but there is now more information to consider based on these new observations.

RMI observations: The Peace Vallis campaign of the Mars Science Laboratory rover (Figure 1) was completed in two phases, the first from sol 1241 to sol 1311 and the second from sol 1981 to sol 2012 [3]. The first set of imagery was acquired from a closer distance; however, the second set was acquired from a better vantage point ~300m higher in elevation (Figure 2). Due to the difference in both elevation and angle to the fan, some targets were deliberately re-imaged to express any variation that might be overlooked with only one image. Additional processing of this imagery adjusted brightness, contrast, and corrected vignetting artifacts from the imaging system [4].

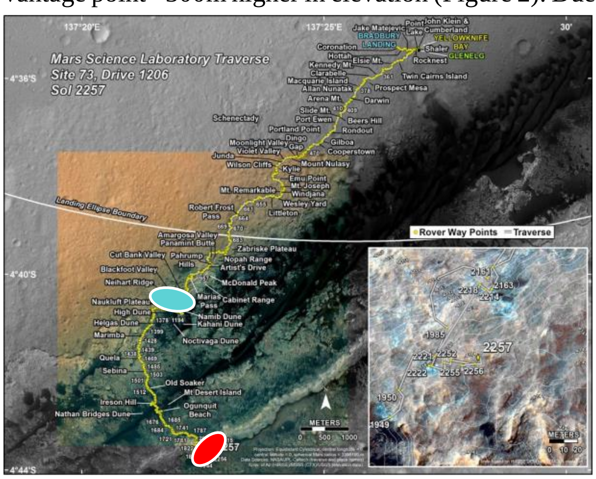

Figure 2. Location of the two phases of the Peace Vallis campaign. Phase 1 outlined in blue, Phase 2 outlined in red.

Orbital data: HiRISE DTM data (1m/px) of the fan illuminate features which are not apparent in visual imagery. Figure 3 is a shaded relief depiction of the fan outlined in red with cool colors representing high elevation and warmer colors representing low elevation.

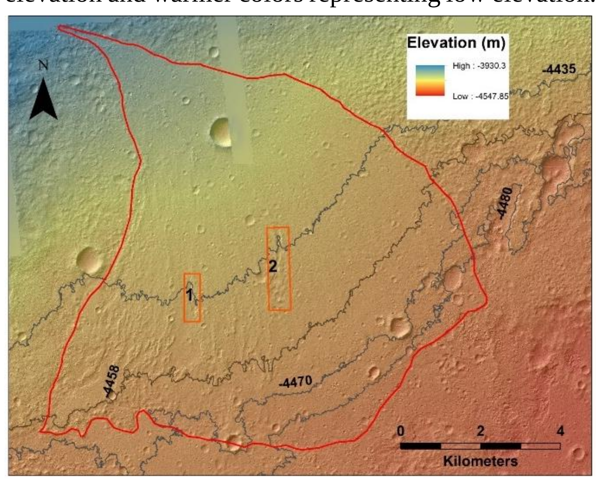

Figure 3. HiRISE DTM shaded relief and elevation data on the Peace Vallis fan (outlined in red).

Discussion: The Peace Vallis fan is a complex, multi-stage system which has been elucidated through the acquisition and study of imagery and data products.

Remnant fan deposits. At the lower section of the Peace Vallis channel there are flat-lying sections of a remnant fan unit that has been subsequently incised and abandoned several tens of meters above the present Peace Vallis channel. These deposits represent a much earlier stage of fan deposition.

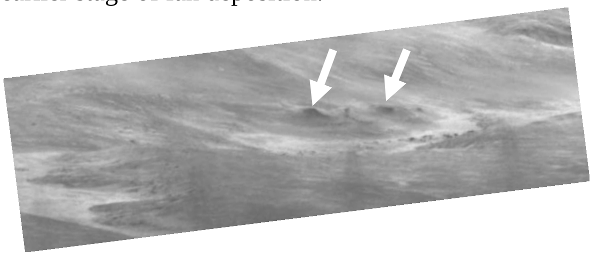

Figure 7. The Peace Vallis channel near the head of the fan (CCAM01011). Arrows indicate the abandoned fan deposits.

Inverted channels. Several features exist on the upper Peace Vallis Fan that resemble inverted fluvial channels like those seen on terrestrial fans and elsewhere on Mars. These resistant ridges were deposited and later exhumed by surface water and wind erosion. Using the ridge height and cratering statistics, a minimum rate of deflation can be calculated.

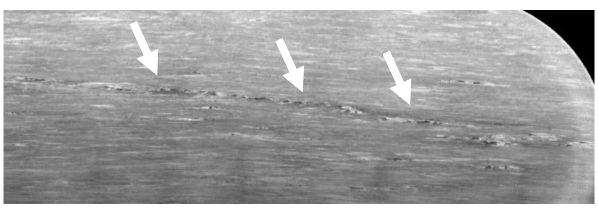

Figure 8. The largest of the inverted channels on the Peace Vallis fan (CCAM03998) indicated by arrows.

AF-BF unit contact. A sharp contact exists between the upper AF (alluvial fan) unit and the lower BF (bedded and fractured) unit. From orbit there is a clear textural difference. In the RMI imagery this contact is seen as a distinct scarp which is most pronounced on the west side of the fan and gradually lessens to the east (Figure 6). The contact can be seen in orbital data at the -4435 elevation contour (Figure 3).

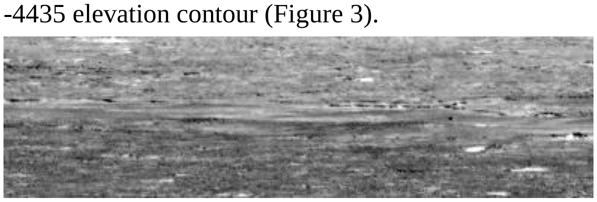

Figure 6. Contact between the lower BF unit and the upper AF unit marked by the scarp in the center of CCAM02984.

Fan asymmetry. The Peace Vallis Fan has a more complex depositional and erosional history than a typical symmetric alluvial fan. The western side of the fan shows a rugged, eroded surface while the eastern side of the fan is relatively smooth (Figure 3). This is due to the thickness of the AF unit on either side. In the west, the AF unit is thin due to subsequent surface and groundwater erosion. The east side did not see the same amount of disruption and therefore is still covered with a relatively thick layer of AF unit obscuring the underlying, rugged BF unit.

Layer continuity. Individual sedimentary beds within the Peace Vallis fan can be followed for 10s of meters. The BF unit contains more of these flat lying beds whereas the AF unit is a fine sediment apron with less structure.

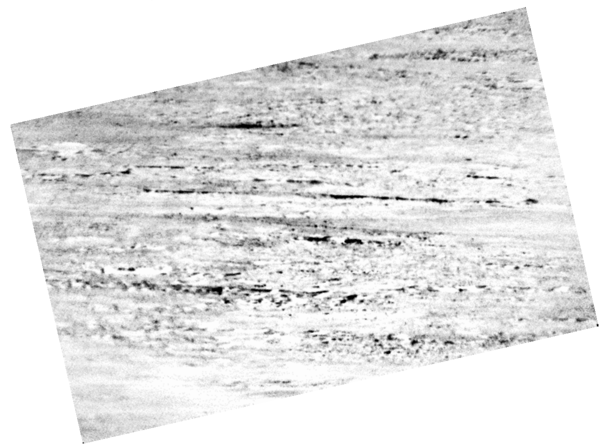

Figure 5. An adjusted edit of CCAM02984 of the fan showing the continuity of individual beds.

Groundwater sapping channels. The Peace Vallis campaign captured a texturally distinct feature ~11.5 km away during the ChemCam RMI 20x1 raster CCAM04981 sequence [3]. Topographic cross-sections across and down the channels reveal a repeating, self-similar morphology characterized by flat bottoms, steep parabolic sides, and an amphitheater-like headwall from continued backwasting. These groundwater springline channels (box 1 & 2 in Figure 3) reside at the -4435 elevation contour which represents a similar morphologic boundary to springlines observed on terrestrial fans [5,6]. These features represent the youngest fluvial event on the surface of the fan.

Conclusions: Understanding of the formation and architecture of the Peace Vallis fan has continued to evolve since the initial mapping efforts before the landing of the Mars Science Laboratory rover. Utilizing orbital HiRISE DTM data and ChemCam RMI imagery from the Peace Vallis campaign, new insights into this complex system begin to emerge.

References: [1] Sumner D. Y. et al. (2013) NTRS. [2] Palucis M. C. et al. (2014) JGR: Planets; 119.4: 705-728. [3] Gallegos Z. G. et al. (2018) *LPSC XLIX*, Abstract #2965. [4] LeMoulic S. et al. (2019) LPSC *L*. [5] Scuderi L. A. et al. (2019) LPSC *L*, abstract# 2714. [6] Scuderi L. A. et al. (2019) *Science*, in submission.